JOURNAL OF OPTOELECTRONICS AND ADVANCED MATERIALS Vol. 12, No. 11, November 2010, p. 2194 - 2198

Temperature and series resistance effect on the forward bias current-voltage (I-V) characteristics of In/p-InP Schottky barrier diode (SBD)

D. KORUCU

Department of Physics, Faculty of Arts and Sciences, Gazi University, 06500 Ankara,Turkey

In this study, the forward bias current-voltage (I-V) characteristics of In/p-InP Schottky Barrier diode (SBD) have been examined in the temperature range of 120-320 K with a temperature step of 40 K. Experimental results show that the values of ideality factor (n) and zero-bias barrier height Φ_{bo} were found strongly temperature dependent and while the value Φ_{bo} increases, the n decreases with increasing temperature. Such behavior of Φ_{bo} and n were interpreted on the basis of the existence of Gaussian distribution (GD) of the barrier heights (BHs) around a mean value due to BH inhomogeneities at metal/semiconductor (M/S) interface. The deviation form lineerity Ln I-V plots in the high bias range was also attributed to series resistance (R_s) effect. In addition, the values of series resistance (R_s) and shunt resistance (R_{sh}) were obtained as a function of temperature and applied bias voltage using Ohm's Law. The values of the R_s and (R_{sh}) were also found strongly temperature and applied bias voltage dependent such that their values increase with increasing temperature and applied bias voltage. The value of R_s decreases with increasing temperature for each temperature and applied bias voltage. The changing of the R_s becomes independent form temperature at high voltage region. Non linear Ln I-V plots at high bias region was due to R_s effect. While the values of R_s, R_{sh} and n decrease, Φ_{bo} and I_o increase with increasing temperature.

(Received September 10, 2010; accepted November 19, 2010)

Keywords: Schottky diodes, I-V-T characteristic, Gaussian distribution, Series and shunt resistance, Barrier inhomogenity

1. Introduction

Indium Phosphat (InP) has gained considerable interest as one of the most promising III-V semiconductors. InP is convenient material for applications in electric and optoelectronic devices due to the direct band gap of 1.35 eV. Metal/InP interfaces play an important role in optoelectronic devices such as infrared detectors and sensors in thermal imaging, solar cells etc. [1-3]. Also InP and its alloys have received increased attention due to the applications in MS, metal-insulator-semiconductors (MIS), MIS field effect transistors (MISFETs), light emitting diodes (LEDs) and solar cells [3-6].

The performance and reliability of such devices is dependent especially on the formation of barrier height (BH) at M/S, series R_s of devices, the distribution of interface states (N_{ss}) at semiconductor/insulator interface. Also, the changes in temperature and applied bias voltage have important effect on the electrical parameters of these devices. There are many investigations in the past five decades [7-10]. Metal/semiconductor contacts were performed by using single crystal mechanism and by observing the effect of shunt and series resistance on the electrical characteristics of the polycrystalline semiconductor devices [10]. The evaluation of forward bias I-V characteristics in SBDs, only at room temperature does not give detail information about the current-transport mechanisms and nature of the BH formed M/S interface. Many researchers have been evaluated in I-V measurements at wide temperature range to understand different aspects of current-conduction mechanism [11-21]. Therefore the forward bias I-V characteristics of the In/p-InP SBD has been investigated in the temperature range of 120-320 K with a temperature step of 20 K.

The current transport mechanisms are dependent on various parameters such as surface preparation processes, inhomogeneity of the BH and insulator layer thickness at the M/S interface, N_{ss} localised insulator/semiconductor interface, R_s of device, impurity concentration of semiconductor and the sample temperature [11-16]. Due the effects of temperature, in SBD structure, the change in main diode parameters such as ideality factor (n), barrier height (Φ_{bo}) at M/S interface, R_s of device are considerably high especially at low temperatures. The changing of Φ_{bo}, n and non linear behaviour of activation energy plots ($\ln(I_o/T^2)$-1/T) especially at low temperature have been explained on Thermionic emission (TE) mechanism with Gaussian distribution (GD) [11-14,16-22]. Distributions of spatial barrier inhomogeneities in M/S or MIS type SBD structure are explained with GD function [23-25]. Therefore, in this study, the forward and reverse bias I-V measurements of In/p-InP Schottky barrier diodes (SBDs) have been investigated in temperature range of 120-320 K.

The experimental results shows a decreasing of n and increasing of Φ_{bo} and R_s values with increasing temperature. The temperature dependence of SBHs characteristics of Sn/p-InP SBDs were interpreted on the basis of the existence of Gaussian distribution (GD) of the BHs around a mean value due to barrier height inhomogeneities prevailing at M/S interface.

2. Experimental procedure

The cleaned and polished half of diameter float zone (100) p-type (Zn doped) single crystal InP having thickness of 350 μm with 4-8x10^{17} cm^{-3} carrier concentration given by the manufacturer were used to fabricate In/p-InP SBDs . Before contact procedure, the p-InP wafer was dipped in 5 H_2SO_4+H_20_2+ H_20 solution for 1.0 min to remove surface damage layer and undesirable impurities and then in H_20+HCl solution and then followed by a rinse in de-ionized water with a resistivity of 18 MΩ cm. In order to prevent undesirable any oxidation the wafer was dried with high-purity nitrogen and inserted into the deposition chamber immediately after etching process. The back side of the p-type InP was formed by sequentially evaporating Zn and Au layers on InP in a vacuum-coating unit of 10^{-6} Torr. After that, low resistance ohmic contact InP wafer was formed by sintering the evaporated Zn and Au layers at 350 °C for 3 min in flowing N_2 in a quartz tube furnace. Finally, the Schottky contacts were formed by evaporating In dots with diameter of about 1mm on the front surface of the p-InP. Fig. 1 shows prepared Schottky contact diagram.

The current-voltage (I-V) characteristics of In/p-InP SBDs were performed by using a Keithley 2400 Sourcemeter. All measurements were carried out in the temperature range of 120-320 K using a temperature controlled Janes vpf-475 cryostat, which enables us to make measurements in the temperature range of 77-450 K. The bias voltage is swept from – 3 to +3 V. The sample temperature was always monitored by use of a copper-constant thermocouple close to the sample and measured with a Keithley model 199 DMM/scanner and Lake Shore model 321 auto-tuning temperature controllers.

3. Results and discussion

Fig. 2., shows the semilogarithmic forward and reverse bias I-V characteristics of In/p-InP SBD at varios temperatures. As can be seen in Fig.2, the forward bias I-V characteristics show a rectifier behavior in the whole temperature. It is clear that the forward bias I-V characteristics at intermediate bias voltage region show a lineer behavior but deviated from linearity at high forward bias voltages due to the effects of series resistance, native interfacial insulator layer, a wide distribution of low BH patches and particular distribution of interface states at M/S interface [4,11,15].

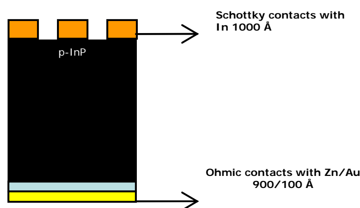

Fig. 1 Prepared In/p-InP Schottky diode structure

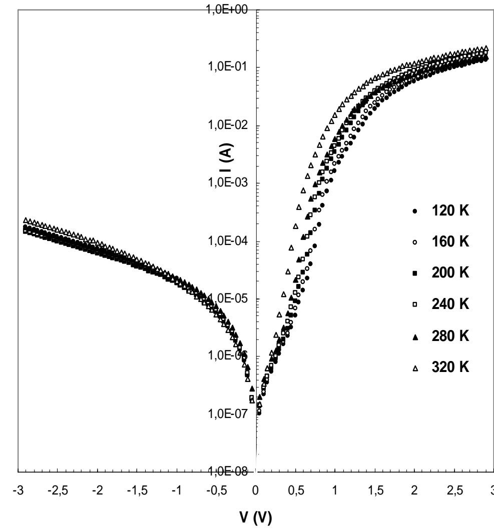

Fig. 2 Temperature-dependent the forwad and reverse bias LnI-V characteristics of the In/p-InP Schottky barrier diode.

when the diode quality factor grater than unity and Rs suficiently high, the relationship between the voltage (V≥3 kT/q) and the current through a barrier at M/S interface, based on thermionic emission theory (TE), can be expresed as [4,26]

$$I = I_0\left[\exp\left(\frac{qV}{n\,kT}\right) - 1\right] + \frac{q(V - IR_s)}{R_{sh}} \tag{1}$$

where I_o is the reverse saturation current, V is the applied voltage on the SBD, n is ideality factor, R_s is the series and R_{sh} is shunt resistance of SBD.

The ideality factor was calculated from the slope of the linear region of the forward bias LnI-V plot and can be written from Eq.(1) as

$$n = \frac{q}{kT}\left(\frac{dV}{dLnI}\right) \tag{2}$$

where dLnI/dV is the slope of linear region of LnI - V plots. The value of Φ_{bo} is calculated from the extrapolated I_o at zero bias according to following equation as

$$\Phi_{Bo} = \frac{kT}{q} Ln\left(\frac{AA^{**}T^2}{I_o}\right) \tag{3}$$

The high values of n can be attributed to a native insulator layer at M/S interface and particular distribution of interface states localized at semiconductor/insulator interface. Because the diode ideality factor greater than unity is generally attributed to the presence of a bias dependent SBH, image forces lowering, generation-recombination or interface recombination, interface impurities, barrier inhomogenity and interfacial insulator layer [11, 27, 28]. As can be seen in Table 1, the values of

n are higher than unity for especially at low temperature. From Table 1, the values of n ranged from 10,36 at 120 K to 2,29 at 320 K. The high values of n is a proof of a deviation from TE theory in the current conduction mechanisms [4,14-20].

Table 1 Temperature dependent values of some SBD parameters determined from forward bias I-V characteristics at various temperature.

T (K)	n	I_o (A)	Φ_{bo} (eV)	$n.\Phi_{bo}$ (eV)
120	10,36	$3,33x10^{-8}$	0,270	1,109
160	6,97	$4,01\ x10^{-8}$	0,357	0,977
200	4,83	$5,00\ x10^{-8}$	0,442	0,828
240	3,61	$6,00\ x10^{-8}$	0,527	0,729
280	2,75	$9,00\ x10^{-8}$	0,605	0,621
320	2,29	$1,52\ x10^{-7}$	0,677	0,558

The changing of n and Φ_{bo} with temperature for the In/p-InP Schottky diode are given in Fig. 3 that is seen the values of n decrease with increasing temperature when the values of Φ_{bo} are increase with increasing temperature. As can be seen in Fig. 4, the ideality factor varies almost linearly with the inverse temperature, such behavior of n is known

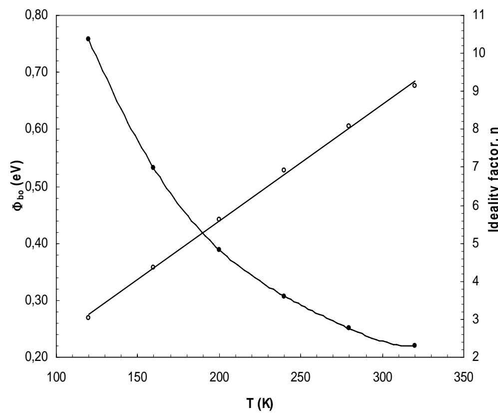

Fig. 3 The temperature dependent of the zero-bias barrier height Φ_{bo} and the ideality factor n of a In/p-InP Schottky barrier diode.

as a T_o anomaly and the temperature dependence of the n can be written as

$$n(T) = n_o + T_o/T \quad (4)$$

where the n_o and T_o are constant which were found to be –2.85 and 1570 K, respectively. In order to evaluate the BH in another way, Richardson plot of the reverse saturation current I_o can be used. By taking the natural logarithm of Equation (2), can be rewritten as

$$\ln\left(\frac{I_0}{T^2}\right) = \ln(AA^*) - \frac{q\,\Phi_{bo}}{kT} \quad (5)$$

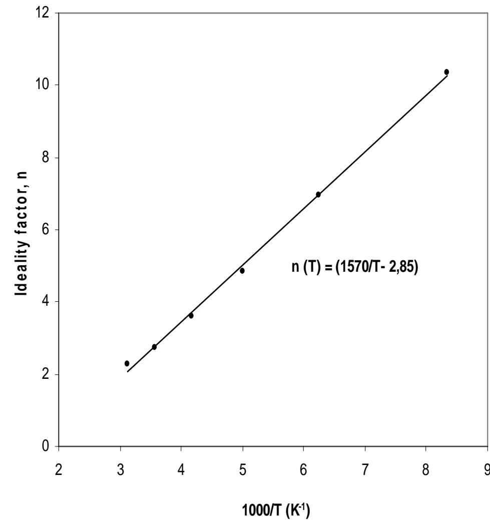

Fig.4 The plots of n - 1000/T of the In/p-InP SBD.

As can be seen in Fig. (5), the conventional Richardson plot of $Ln(I_o/T^2)$ vs 1/T was found to non-linear especially at low temperature range (T ≤ 200 K). On the other hand, the $Ln(I_o/T^2)$ vs 1/nT plot show a good linear behavior in the whole temperature range measured. The deviation in the conventional Richardson plots ($Ln(I_o/T^2)$ vs 1/T) at low temperatures may be due to the spatial inhomogeneous BH and potential fluctuations at the interface that consist of low and high barrier areas[16-21]. Similar results have also been found in the literature [6,11-21]. When the experimental data are fitted between the temperature ranges of 120-320 K in Fig. 5 asymptotically with a straight line, it yields activation energy of 0.513 eV. Likewise, a Richardson constant (A^*) value of $4.51x10^{-8}$ A cm^{-2} K^{-2} for the Sn/p-InP SBD was determined from the intercept at the ordinate of the $Ln(I_o/T^2)$ vs 1/T plot. This value of the A^* is much lower then the known value of 60 A cm^{-2} K^{-2} for holes in Zn doped InP [4]. In Ref. [23] reported that the value of A^* may be affected by the lateral inhomogeneity of the barrier height. On the other hand Song et al. [1] suggested that the rectifier contact area A consists of many sub-areas, each having a definite BH and and a definite area a being isolated from each other. Also, they show that in SB contacts variations of the BH over the contact area can occur as a result of inhomogeities in the interfacial oxide layer composition, nonuniformity of the native interfacial layer thickness and distributions of interfacial charges [11,19,21-29]. As can be seen Table 1 and Fig.6, the value of effective BH ($n\Phi_{bo}=\Phi_{Beff.}$) decrease with increasing temperature according with the temperature dependent bandgap of semiconductor as

$$\Phi_{Beff.} = \Phi_{bo}(0\ K) - \alpha\ T \qquad (6)$$

Where $\Phi_{bo}(0\ K)$ is the BH at zero-temperature and α is temperure coefficient of BH. The values of $\Phi_{bo}(0\ K)$ α are found as 1.419 eV and $-28x10^{-4}$ eV/K, respectively. The value of temperure coefficient of BH is close to the negative temperature coefficient of InP bandgap.

Due to the deviation of Ln I-V slope from lineer at high voltage region the bias voltage dependent series resistance profile of In/p-InP SBD was obtained from the I-V data using Ohm Law ($\delta V_i/\delta I_i$) and are given in Fig. 7 (a). it can be seen clearly in Fig. 7 (a), the values of resistance are decreased with increasing voltage and the value of series resistance is almost independent from bias voltage at sufficiently high forward bias region. On the other hand the series resistance is independent of bias voltage for sufficiently high reverse bias region, which is equal to the diode shunt resistance, R_{sh}. While the values of resistance at high bias voltage are series resistance, shunt resistance is to be found at low bias region [4, 26]. From Fig. 7 (a), the values of R_s and R_{sh} for 120 and 320 K have been calculated as a 18.1 Ω, 0.48 MΩ and 12.57 Ω, 0.3 M Ω, respectively. As can be seen in Fig. 7 (b), the value of series resistance decrease with increasing temperature and are show strongly voltage dependent.

It is clear vthat the values of R_s and R_{sh} were found strongly dependent on the temperature and applied bias voltage and decrease with the increasing temperature. Such behaviour of R_s and R_{sh} can be explained by the enhanced conductivity of the InP and it is an expected behaviour. Also these values of R_s and R_{sh} are valid for the fabrication of semiconductor devices.

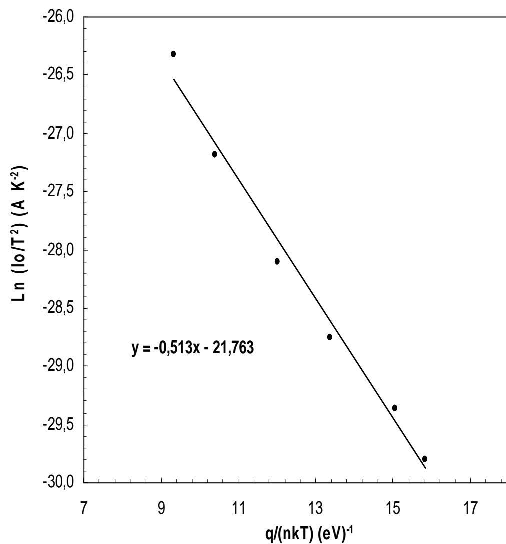

Fig. 5. Richardson plots of the $\ln(I_o/T^2)$ -1/nT for In/p-InP Schottky barrier diode.

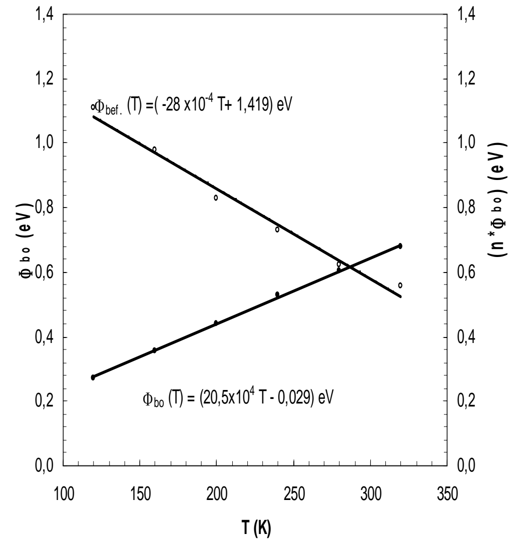

Fig.6. Temperature dependent values of $\Phi_{Beff.}$ and Φ_{bo} for In/p-InP Schottky barrier diode.

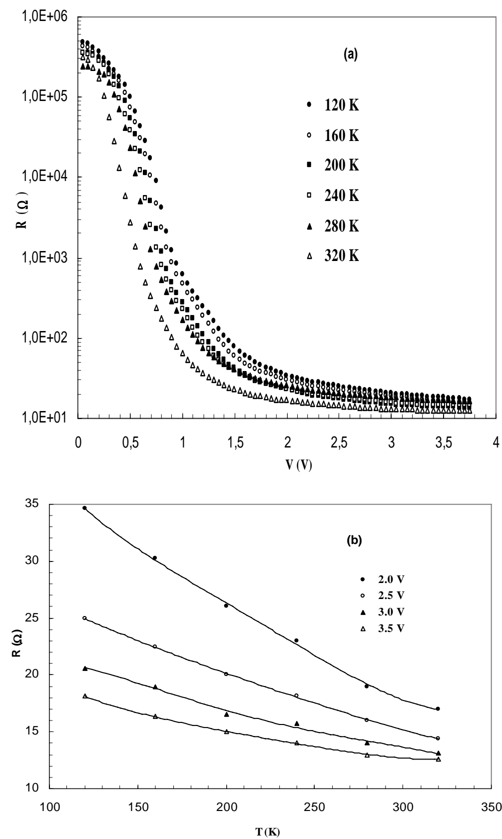

Fig. 7 The variation of the resistivity of In/p-InP SBD (a) as a function of voltage in the wide temperature range (b) as the temperature dependent of R_s at the different voltage ranged from 2 to 3.5 V, respectively.

4. Conclusions

The forward and reverse bias I-V measurements of In/p-InP SBD have been carried out in the temperature range of 120-320 K. From experimental results, prepared In/InP SBD has shown a good rectifier behaviour. The LnI-V plots show a linear behaviour at intermediate forward bias voltage for each temperature but deviated from the linearity at high voltage region due to series resistance effect. The value of R_s decreases with increasing temperature for each temperature and applied bias voltage. The changing of the R_s becomes independent form temperature at high voltage region. So the resistance which corresponds to the high voltage region is named as R_s whereas the resistance corresponding to the low voltage low voltage region is R_{sh}. It is clear that the main electrical parameters such as I_o, n, Φ_{bo}, R_s and R_{sh} obtained from I-V data were found strongly dependent on the temperature and applied bias voltage. The deviation form lineerity in the Ln I-V plots at high bias range was also attributed to R_s effect. While the values of R_s, R_{sh} and n decrease, Φ_{bo} and I_o increase with increasing temperature. Such behaviour of Φ_{bo} and n with temperature were interpreted on the basis of the existence of Gaussian distribution (GD) of the BHs around a mean value of BH due to BH inhomogeneities at metal/semiconductor (M/S) interface.

References

[1] Y. P. Song, R. L. Van Meirhaeghe, W.H. Laflere, F. Cardon, Solid-State Electron., **29**, 663 (1986).
[2] A. Ahaitouf, A. Bath, E. Losson, E. Abarkan, Mater. Sci. and Eng.**B52**, 208 (1998).
[3] M. Yamaguchi, A. Khan, N. Dharmarasu, Solar Energy Materials & Solar Cells. **75**, 285 (2003).
[4] S.M. Sze, Physics Semiconductor Devices, John Wiley and Sons, New York, (1981).
[5] T.S. Huang, R.S. Fang, Solid State Electron., **37**, 1661 (1994).
[6] H. Çetin, E. Ayyildiz, Appl. Surf. Sci., 253 (2007).
[7] M.K. Bera, S.Chakraborty, S.Saha, D. Paramanik, S. Varma, S. Bhattacharya, C.K. Maiti, Thin Solid Film. **504**, 183 (2006).
[8] N. Konofaos, E.K. Evangelou, Semicond. Sci. Technol. **18**, 56 (2003).
[9] N. Konofaos, E.K.Evangelou, Z. Wang, V. Kugler, U. Helmersson, Journal of Non-Crystalline Solids**.,** **303**, 185 (2002).
[10] L. A. Kosyachenko, X. Mathew, V. V. Motushchuk, V. M. Sklyarchuk, Solar Energy, **80,** 148 (2006).
[11] Ş. Karataş, Ş. Altındal, A. Türüt, A. Özmen, Appl. Surf. Sci., **217**, 250 (2003).
[12] H. Kanbur, Ş. Altındal, A. Tataroğlu, Appl. Surf. Sci., **252**, 1732 (2005).
[13] Ş. Altındal, A. Tataroğlu, İ. Dökme, Solar Energy Mater. and Solar Cells, **85**, 345 (2005).
[14] S. Chand, J. Kumar, Semicond. Sci. Technol., **10,** 1680 (1995).
[15] F. Yakuphanoglu, Physica B, **388**, 226 (2007).
[16] D. E. Yıldız, Ş. Altındal, Microelectronic Engineering, 85, 289 (2008).
[17] İ. Dökme, Ş.Altindal, M.M. Bülbül, Applied Surface Science, Vol. 252, 7749 (2006).
[18] A. Tataroğlu, Ş. Altındal, Journal of Alloys and Compounds, Vol. 484, 405(2009).
[19] S. Zeyrek, Ş. Altındal, H. Yüzer, M. M. Bülbül, Applied Surface Science, **252**, 2999 (2006).
[20] S. Demirezen, S. Altındal, Current Appl. Physics, **10**, 1188 (2010).
[21] M. Biber, C. Coşkun, A. Türüt, J.Appl. Phys., **31**, 79 (2005).
[22] S. Chand ,J.Kumar, Semicond. Sci.Technol. **11**, 1203 (1996).
[23] P. Cova, A. Sing, Solid State Electron, **33**,11 (1990).
[24] R.T. Tung, Phys. Rev. **B45**, 13509 (1992).
[25] W. Mönch, J. Vac. Sci. Technol. **B17**, 1867 (1990).
[26] A. A .M Farag, E.A.A El-Shazly, M. Abdel Rafea, A. Ibrahim, Solar Energy Materials&Solar Cell, 1853 (2009).
[27]Zs.J. Horvarth, Solid-State Electron., **39**, 176 (1996).
[28] Ş. Karataş, Ş. Altındal, M. Çakar, Physica B: Condensed Matter, **357**(3-4), 386 (2005).
[29] Ş. Karataş, Ş. Altındal, Materials Science and Engineering: B, **122**(2), 133 (2005).

Corresponding author: dkorucu@yahoo.com